MEASUREMENT OF PROTEIN ROTATIONAL MOTION USING FREQUENCY DOMAIN POLARIZED FLUORESCENCE DEPLETION

THOMAS M. YOSHIDA, FAHIMEH ZARRIN, AND B. GEORGE BARISAS
Department of Chemistry, Colorado State University, Fort Collins, Colorado 80523

ABSTRACT Polarized fluorescence depletion (PFD) methods (Yoshida, T. M. and B. G. Barisas. *Biophys. J.* 1986. 50:41–53) are ~10^3–10^4 fold more sensitive than other techniques for measuring protein rotational motions in cell membranes and other viscous environments. Proteins labeled with fluorophores having a high quantum yield for triplet formation are examined anaerobically in a fluorescence microscope. In time domain PFD experiments a several-microsecond pulse of linearly polarized light produces an orientationally-asymmetric depletion of ground state fluorescence in the sample. Monitoring the decay of ground state depletion with a probe beam alternatively polarized, parallel, and perpendicular to the depletion pulse permits the triplet lifetime and rotational correlation time to be resolved and evaluated. We have now explored fluorescence depletion methods in the frequency domain to see whether such measurements could provide simpler and more efficient routine measurements of protein rotational relaxation than previous time domain PFD methods. An acousto-optic modulator (AOM) modulates the intensity of a 514.5 nm argon ion laser beam and a Pockels cell (PC) rotates its plane of polarization. These devices are driven by sinusoidal or square waves in fixed frequency relation, and rigidly phase locked, one to another. The fluorescence emitted from a sample then contains various overtones and combinations of the AOM and PC frequencies. The magnitude and phase of individual fluorescence signal frequencies are measured by a lock-in amplifier using a reference also phase-locked to both the AOM and PC. Specific frequencies permit evaluation of the rotational correlation time of the macromolecule and of the fluorophore triplet state lifetime, respectively. Measurement of bovine serum albumin rotation in glycerol solutions by this method is described.

INTRODUCTION

A technique has been developed to measure slow rotational motions of proteins and other macromolecules in viscous environments using frequency domain polarized fluorescence depletion (FPFD). Frequency domain techniques have long been used to measure fluorescence lifetimes of intrinsic protein fluorophores and of fluorescent probes and labels (for reviews see Jameson et al., 1984 and Gratton et al., 1984). More recently, measurements of nanosecond rotational relaxation of fluorescent probes in solution (Mantulin and Weber, 1977; Valeur and Weber, 1977), in artificial lipid bilayers (Lakowicz and Prendergast, 1978; Lakowicz et al., 1979; Lakowicz and Thompson, 1983; Lakowicz et al., 1985) and in biological membranes (Weber et al., 1976; Chong et al., 1983) have been reported. Although time domain techniques remain in common use, frequency domain techniques have become increasingly attractive because of reduced analysis time and their potential to resolve multiple excited state decay processes in heterogeneous samples (Jameson et al., 1984; Keating-Nakamoto et al., 1985; Gratton and Jameson, 1985). Also by eliminating the excitation pulse used in time domain experiments, much shorter excited state processes can be measured without complicated data deconvolution. Frequency domain techniques have also been applied to field of phosphorimetry (Garland and Birmingham, 1986). Mousa and Winefordner (1974) introduced the theory and technique of phase-resolved phosphorimetry and applied it to the analysis of a binary mixture of phosphors in solution.

We have explored frequency domain PFD measurements of macromolecular rotational relaxation on the microsecond to millisecond time scale, this time scale being appropriate for motions of proteins in biological membranes (Cherry, 1979). In a previous paper (Yoshida and Barisas, 1986) we described the theory and instrumentation for measuring slow rotational motion of proteins in viscous environments using time domain polarized fluorescence depletion (PFD). This technique utilizes the relatively long lifetime of the excited triplet state and, by

Address all correspondence to Dr. Barisas.
Dr. Zarrin's present address is Bristol-Myers U.S. Pharmaceutical and Nutritional Group, Evansville, IN 47721

detecting depletion of ground state fluorescence, has far more sensitivity than other techniques which rely on detection of low quantum yield phosphorescence (Austin et al., 1979; Moore et al., 1979; Garland and Moore, 1979). This makes PFD highly attractive for measurements on biological samples.

In time domain PFD, a protein labeled with a fluorescent dye having a significant quantum yield for triplet formation is examined anaerobically and exposed to a short, high intensity pulse of linearly polarized light. The pulse produces an anisotropic depletion of ground state fluorescence which is measured by a low intensity probe beam. Time evolutions of fluorescence alternately polarized parallel and perpendicular to the depletion pulse are recorded by signal averaging. Simple equations modeling the time evolution of this fluorescence depletion were developed for various systems of interest and these equations allow direct evaluation of the triplet lifetime and rotational correlation time from experimental data.

Frequency domain PFD uses the same microscope-based optical system as does the time domain technique but relies on a different means of depleting ground state fluorescence and of collecting and analyzing the data. In frequency domain PFD, rather than using an impulse function to create ground state depletion, both the intensity and polarization of the light are continuously modulated by sine or square waves at two different fixed frequencies. If the two frequencies are rigidly phased locked each to the other, the frequency spectrum of the fluorescence signal contains overtones and combinations of these two fundamental frequencies. Some of these frequencies are strongly dependent on the triplet lifetime and others on the rotational correlation time. Each signal has a frequency-dependent phase shift and magnitude which can be measured as functions of frequency by using phase sensitive detection. From this information and from equations developed to model the process, the fluorophore triplet lifetime and rotational correlation time can be calculated.

There are two major motivations for developing FPFD. The first is to explore the possibility of simplified instrumentation for rotational motion measurements. The second is to use the limited amount of data available in PFD experiments more efficiently. By eliminating the high intensity pulses used in time domain PFD to achieve ground state depletion, the need for high-speed timing controllers and PMT gating circuits is avoided. Eliminating the depletion pulse also offers the possibility of measuring submicrosecond rotational motions without the need for nanosecond pulsed lasers. Time domain PFD also requires high speed signal averaging. Time resolution must be adequate to delineate rotational motion on the submicrosecond timescale and such signal processors are complex and expensive. In FPFD a lock-in amplifier replaces the signal averager. Moreover, by proper choice of the two drive frequencies in the frequency domain technique, signals containing rotational information can be optically heterodyned to a quiet region of the spectrum as much as an order of magnitude below any of the drive frequencies and their overtones, thus further simplifying signal acquisition.

Here we present the theory for both sine wave and square wave-modulated FPFD and describe the instrumentation developed to implement the square wave technique. We also present results of the measurement of rotational motion of bovine serum albumin (BSA) in glycerol using both frequency domain and time domain PFD.

GLOSSARY

$L(v, t)$	light intensity function
$\bar{I}$	average modulated excitation intensity
A	extent of intensity modulation
v	intensity modulation frequency
I_0	unmodulated source intensity
$R(\theta, \phi, w, t)$	light polarization function
w	polarization modulation frequency
θ, ϕ	sample coordinate angles
$P(\theta, \phi, v, w, t)$	light function
P_0, P_2, P_2^2	associated Legendre polynomials in cos θ.
$S(\theta, \phi, t)$	distribution function for singlet molecules
D	rotational diffusion coefficient
∇^2	Laplacian operator
k_t	first order rate constant for triplet decay
k_r	rate constant for rotational relaxation
k_c	combined rate constant for triplet decay and rotational relaxation
τ_t	triplet lifetime
τ_r	rotational correlation time
β	chromophore depletion constant
λ	wavelength of light
ϵ	molar absorptivity
Φ_t	quantum yield for triplet formation
N	Avogadro's number
c	speed of light
h	Planck's constant
$I(v, w, t)$	time-dependent fluorescence intensity
B	system gain constant
g	lock-in amplifier gain
E	efficiency of photon collection
f	number of illuminated chromophores
Φ_c	quantum efficiency for the PMT photocathode
M_{2v}	sine wave-modulated lifetime-dependent signal magnitude
ϕ_{2v}	sine wave-modulated lifetime-dependent phase
$M_{2(v-w)}$	sine wave-modulated rotation-dependent magnitude
$\phi_{2(v-w)}$	sine wave-modulated rotation-dependent phase
$E(t)$	lock-in amplifier reference voltage function
$D(t)$	lock-in amplifier demodulator function
U_{2v}	steady-state voltage for lifetime-dependent signal
$U_{2(v-w)}$	steady-state voltage for rotation-dependent signal
T	measurement period
P	Gaussian laser beam power
w	laser beam $1/e^2$ radius
σ	spatial concentration of chromophores in the sample

THEORY

The simplest system to consider is a spherical particle with a single, rigidly-attached dye molecule, situated at the origin of a right-handed *xyz*-coordinate system and rotating in a three-dimensional isotropic medium. The absorption transition dipole moment of the dye is described by angles θ and ϕ and is assumed to be parallel to the emission transition moment, which is a reasonable assumption for EITC (Cherry and Schneider, 1976). Abundant work on triplet spectroscopy (see, for example, Austin et al., 1979), as well as our previous time domain PFD studies (Yoshida and Barisas, 1986), demonstrates that dyes such as EITC are converted to the triplet state with a first-order rate constant proportional to light intensity and decay to the singlet state by one or more first-order processes. For simplicity it is assumed that the fluorophore exhibits a single exponential triplet decay and that the triplet lifetime is much greater than the rotational correlation time.

Sine Wave Modulation

The excitation light $L(v, t)$ is sine wave-modulated at a frequency v and travels along the x-axis.

$$L(v, t) = \bar{I}(1 + A \cos vt), \tag{1}$$

where $\bar{I}$ is the average modulated excitation intensity and $0 \leq A \leq 1$ is the extent of intensity modulation by the acousto-optic modulator. It should be noted that, when high extents of modulation are attempted with such devices, their transfer functions become nonlinear in applied drive voltage. $\bar{I}$ is in turn given by $\bar{I} = I_0/(1 + A)$ where I_0 is the unmodulated source intensity. The polarization of the light $R(\theta, \phi, w, t)$ is modulated at a different frequency w, where

$$R(\theta, \phi, w, t) = \cos^2\theta \sin^2(wt/2) + \sin^2\theta \cos^2\phi \cos^2(wt/2). \tag{2}$$

The first term in Eq. 2 represents the polarization component parallel to the z-axis (*vertical*) and the second term is the component parallel to the y-axis (*horizontal*). Experimentally Eq. 2 can be realized by modulating a Pockels cell at frequency w with a triangular wave ranging between zero volts and the half-wave voltage of the Pockels cell. Fluorescence emission is collected at 180° with respect to the excitation beam along the x-axis and no polarization analyzer is used in the detection optics.

The light function $P(\theta, \phi, v, w, t)$ is expressed as the product of the light intensity and polarization functions, giving

$$P(\theta, \phi, v, w, t) = L(v, t)R(\theta, \phi, w, t). \tag{3}$$

Substituting Eqs. 1 and 2 and expressing the spatial variables in Legendre polynomials in $\cos\theta$, Eq. 3 can be expanded to

$$\begin{aligned} P(\theta, \phi, v, w, t) = \frac{1}{6}\bar{I}\Big[&2P_0 + 2AP_0 \cos vt \\ &+ P_2 + AP_2 \cos vt - 3P_2 \cos wt \\ &- \frac{3A}{2}P_2 \cos(v + w)t \\ &- \frac{3A}{2}P_2 \cos(v - w)t \\ &+ \frac{1}{2}P_2^2 \cos 2\phi + \frac{A}{2}P_2^2 \cos 2\phi \\ &\cdot \cos vt + \frac{1}{2}P_2^2 \cos 2\phi \cos wt \\ &+ \frac{A}{4}P_2^2 \cos 2\phi \cos(v + w)t \\ &+ \frac{A}{4}P_2^2 \cos 2\phi \cos(v - w)t\Big], \end{aligned} \tag{4}$$

where P_0, P_2, and P_2^2 are the associated Legendre polynomials in $\cos\theta$.

Given the assumptions stated at the beginning of this section, the diffusion equation in three dimensions is

$$D\nabla^2 S(\theta, \phi, t) + k_\ell\left[\frac{1}{4\pi} - S(\theta, \phi, t)\right] - \beta P(\theta, \phi, v, w, t)S(\theta, \phi, t) = \frac{\partial S(\theta, \phi, t)}{\partial t}, \tag{5}$$

where $S(\theta, \phi, t)$ is the distribution function for molecules in the singlet state, D is the rotational diffusion coefficient, ∇^2 is the Laplacian operator, k_ℓ is the first order rate constant for triplet decay, and β is a constant dependent on the molar absorptivity of the chromophore where

$$\beta = \frac{6{,}909\,\epsilon\,\lambda}{h\,c\,N}\Phi_t, \tag{6}$$

where λ is the wavelength of light, ϵ is the molar absorptivity for the fluorophore, Φ_t is the quantum yield for triplet formation, N is Avogadro's number, c is the speed of light, and h is Planck's constant.

The diffusion equation is readily solved when the extent of ground state depletion is small. In this limiting case the distribution function can be expressed as a finite sum of discrete frequencies

$$S(\theta, \phi, t) = \frac{1}{4\pi}\Big[a_0 + \sum(a_j \cos jt + b_j \sin jt)\Big], \tag{7}$$

where a_j and b_j are coefficients depending only on the spatial variables. The values of j represent temporal frequencies in the distribution function which are uniquely

determined by the form of the excitation function. For the particular excitation function described by Eq. 4, the allowed values of j are v, the AOM fundamental frequency; w, the polarization modulation frequency; and the combinations of these frequencies, $v + w$ and $v - w$.

The solution to the diffusion equation can be found by substituting Eqs. 4 and 7 into the diffusion equation giving the coefficients below. Although we immediately convolve these terms with the light function to obtain the time-dependent fluorescence intensity signal, we include them here for the use of readers who may wish to vary the detection geometry, add an emission polarizer, etc.

$$a_0 = 1 - \frac{1}{3k_\ell}\bar{I}\beta P_0 - \frac{1}{6k_c}\bar{I}\beta P_2 - \frac{1}{12k_c}\bar{I}\beta P_2^2 \cos 2\phi \quad (8)$$

$$a_v = -\frac{1}{3}A\bar{I}\beta\left(\frac{k_\ell}{k_\ell^2 + v^2}\right)P_0 - \frac{1}{6}A\bar{I}\beta\left(\frac{k_c}{k_c^2 + v^2}\right)P_2 - \frac{1}{12}A\bar{I}\beta\left(\frac{k_c}{k_c^2 + v^2}\right)P_2^2 \cos 2\phi \quad (9)$$

$$b_v = -\frac{1}{3}A\bar{I}\beta\left(\frac{v}{k_\ell^2 + v^2}\right)P_0 - \frac{1}{6}A\bar{I}\beta\left(\frac{v}{k_c^2 + v^2}\right)P_2 - \frac{1}{12}A\bar{I}\beta\left(\frac{v}{k_c^2 + v^2}\right)P_2^2 \cos 2\phi \quad (10)$$

$$a_w = \frac{1}{2}\bar{I}\beta\left(\frac{k_c}{k_c^2 + w^2}\right)P_2 - \frac{1}{12}\bar{I}\beta\left(\frac{k_c}{k_c^2 + w^2}\right)P_2^2 \cos 2\phi \quad (11)$$

$$b_w = \frac{1}{2}\bar{I}\beta\left(\frac{w}{k_c^2 + w^2}\right)P_2 - \frac{1}{12}\bar{I}\beta\left(\frac{w}{k_c^2 + w^2}\right)P_2^2 \cos 2\phi \quad (12)$$

$$a_{v+w} = \frac{1}{4}A\bar{I}\beta\left[\frac{k_c}{k_c^2 + (v + w)^2}\right]P_2 - \frac{1}{24}A\bar{I}\beta\left[\frac{k_c}{k_c^2 + (v + w)^2}\right]P_2^2 \cos 2\phi \quad (13)$$

$$b_{v+w} = \frac{1}{4}A\bar{I}\beta\left[\frac{v + w}{k_c^2 + (v + w)^2}\right]P_2 - \frac{1}{24}A\bar{I}\beta\left[\frac{v + w}{k_c^2 + (v + w)^2}\right]P_2^2 \cos 2\phi \quad (14)$$

$$a_{v-w} = \frac{1}{4}A\bar{I}\beta\left[\frac{k_c}{k_c^2 + (v - w)^2}\right]P_2 - \frac{1}{24}A\bar{I}\beta\left[\frac{k_c}{k_c^2 + (v - w)^2}\right]P_2^2 \cos 2\phi \quad (15)$$

$$b_{v-w} = \frac{1}{4}A\bar{I}\beta\left[\frac{v - w}{k_c^2 + (v - w)^2}\right]P_2 - \frac{1}{24}A\bar{I}\beta\left[\frac{v - w}{k_c^2 + (v - w)^2}\right]P_2^2 \cos 2\phi. \quad (16)$$

The combined rate constant k_c for triplet decay and rotational relaxation equals $k_\ell + k_r$. In turn, the rate constant k_ℓ for triplet decay equals $1/\tau_\ell$, where τ_ℓ is the triplet lifetime, and the rate constant k_r for rotational relaxation equals $1/\tau_r$, where τ_r is the rotational correlation time. For a spherical particle in an isotropic medium $\tau_r = 1/6D$.

To solve for the time-dependent fluorescence intensity signal $I(v, w, t)$ the distribution function from Eq. 7 is convolved with the light function from Eq. 4 and the result is again expressed in terms of a Fourier series.

$$I(v, w, t) = Bf \iint S(\theta, \phi, t)\, P(\theta, \phi, v, w, t) \sin\theta \, d\theta \, d\phi \quad (17)$$

$$= Bf[a_0 + \Sigma\,(a_j \cos jt + b_j \sin jt)]. \quad (18)$$

In Eqs. 17 and 18 f is the number of chromophores illuminated and B is defined as

$$B = 6{,}909\, g\, E\, \Phi_c\, \Phi_t\, \epsilon \frac{\lambda}{h\, c\, N}, \quad (19)$$

where g is the amplifier gain, E is the efficiency of photon collection, Φ_c is the quantum efficiency for the PMT photocathode, and the other terms have been previously defined.

In the process of convolving the distribution and light functions, the Legendre coefficients for the frequencies $j = w$ and $j = v \pm w$ sum to zero, but cross terms of the individual coefficients produce new frequencies at $j = 2v$, $j = 2w$ and $j = 2(v \pm w)$. After convolution the Fourier coefficients for the fluorescence signal are as follows:

$$a_0 = \frac{1}{3}\bar{I} - \frac{1}{9}\bar{I}^2\beta\left(\frac{1}{k_\ell} + \frac{1}{5k_c}\right) \quad (20)$$

$$a_v = \frac{1}{3}\bar{I}A - \frac{1}{9}\bar{I}^2A\beta\left[\frac{1}{k_\ell} + \frac{1}{5k_c} + \frac{k_\ell}{k_\ell^2 + v^2} + \frac{k_c}{5(k_c^2 + v^2)}\right] \quad (21)$$

$$b_v = -\frac{1}{9}\bar{I}^2A\beta\left[\frac{v}{k_\ell^2 + v^2} + \frac{v}{5(k_c^2 + v^2)}\right] \quad (22)$$

$$a_{2v} = -\frac{1}{18}\bar{I}^2A^2\beta\left[\frac{k_\ell}{k_\ell^2 + v^2} + \frac{k_c}{5(k_c^2 + v^2)}\right] \quad (23)$$

$$b_{2v} = -\frac{1}{18}\bar{I}^2A^2\beta\left[\frac{v}{k_\ell^2 + v^2} + \frac{v}{5(k_c^2 + v^2)}\right] \quad (24)$$

$$a_{2w} = -\frac{1}{30}\bar{I}^2\beta\left(\frac{k_c}{k_c^2 + w^2}\right) \quad (25)$$

$$b_{2w} = -\frac{1}{30}\bar{I}^2\beta\left(\frac{w}{k_c^2 + w^2}\right) \quad (26)$$

$$a_{2(v+w)} = -\frac{1}{120}\bar{I}^2A^2\beta\left[\frac{k_c}{k_c^2 + (v + w)^2}\right] \quad (27)$$

$$b_{2(v+w)} = -\frac{1}{120}\bar{I}^2A^2\beta\left[\frac{v + w}{k_c^2 + (v + w)^2}\right] \quad (28)$$

$$a_{2(v-w)} = -\frac{1}{120}\bar{I}^2A^2\beta\left[\frac{k_c}{k_c^2 + (v - w)^2}\right] \quad (29)$$

$$b_{2(v-w)} = -\frac{1}{120}\bar{I}^2A^2\beta\left[\frac{v-w}{k_c^2+(v-w)^2}\right]. \quad (30)$$

As can be seen from Eqs. 20–30 the Fourier spectrum of the fluorescence signal is composed of various components which depend on the triplet lifetime and the rotational correlation time. For evaluation of the triplet lifetime the most appropriate frequency to choose is $2v$, since this signal does not contain a term independent of the intensity modulation frequency as does v. Since the intensity and phase of this fluorescence signal are independent of the polarization of the exciting light, it is clearly advantageous to leave the PC off while triplet lifetime data are being collected. We observe that the rate constant for triplet decay is often much smaller than the rate constant for rotational relaxation. In such a case Eqs. 23 and 24 can be simplified to

$$a_{2v} = -\frac{1}{18}\bar{I}^2A^2\beta\left(\frac{k_\ell}{k_\ell^2+v^2}\right) \quad (31)$$

$$b_{2v} = -\frac{1}{18}\bar{I}^2A^2\beta\left(\frac{v}{k_\ell^2+v^2}\right). \quad (32)$$

Eq. 32 corresponds to the in-phase component of the signal with respect to a reference signal of $\sin 2vt$ and Eq. 31 corresponds to the quadrature or the component leading the reference by 90°. The magnitude M_{2v} and phase ϕ_{2v} of the $2v$ signal as functions of acousto-optic modulator (AOM) modulation frequency are

$$M_{2v} = \frac{1}{18}\bar{I}^2A^2\beta Bf\frac{1}{\sqrt{k_\ell^2+v^2}} \quad (33)$$

and

$$\phi_{2v} = \text{ArcTan}\,(v/k_\ell). \quad (34)$$

Eqs. 33 and 34 show that, at low frequencies, the signal tracks the exciting light so its phase shift is zero and its magnitude is proportional to the triplet lifetime. At higher frequencies the signal begins to lead the probe beam because of the finite lifetime of the triplet state. As the frequency increases further, the signal leads the exciting light by 90° and its magnitude decreases as $1/v$.

As can be seen from Eqs. 25–30 the rotational correlation time appears strongly in the second harmonics of the PC frequency and of the sum and difference of the PC and AOM frequencies. Any one of these frequencies could be isolated for determining the combined rate constant k_c. The most promising frequency to choose for this purpose is $j = 2(v-w)$. By choosing v and w relatively close together, rotational information in this frequency is optically heterodyned into a quiet region of the spectrum as much as an order of magnitude below the drive frequencies and their overtones. This simplifies detection considerably as well as improving signal quality. For the $2(v-w)$ terms the magnitude $M_{2(v-w)}$ and phase $\phi_{2(v-w)}$ of the signal are given by

$$M_{2(v-w)} = \frac{1}{120}\bar{I}^2A^2\beta Bf\frac{1}{\sqrt{k_c^2+(v-w)^2}} \quad (35)$$

$$\phi_{2(v-w)} = \text{ArcTan}\left(\frac{v-w}{k_c}\right). \quad (36)$$

It should be noted that v and w always have a fixed frequency ratio dependent on the particular experimental setup and the combined frequency $2(v-w)$ is varied.

It is thus clear that the triplet lifetime and rotational correlation time can be extracted relatively simply from sine wave-modulated FPFD data where the magnitude and phase of a particular fluorescence signal has been measured as a function of its frequency. The magnitude and phase of the rotation-dependent fluorescence signal at $2(v-w)$ are plotted versus $2(v-w)$ in Fig. 1 for three values of τ_r as calculated from Eqs. 35 and 36. Fig. 1 shows that the effect of changing the value of τ_r is to shift the phase angle observed at a particular frequency without significantly changing the general shape of the curve. Similar curves appear in excited state lifetime measurements at the $2v$ frequency. Therefore, once the relations between k_ℓ and k_c and the frequency dependence of fluorescence phase shifts have been experimentally determined for a particular system, phase angle measurements for an unknown sample at the $2v$ and $2(v-w)$ frequencies are all that is required to determine the triplet lifetime and the rotational correlation time within a limited range of values.

Although determination of excited state lifetimes by this method bears some analogy to phase fluorometry (Lakowicz and Maliwal, 1985; Gratton et al., 1984), the two

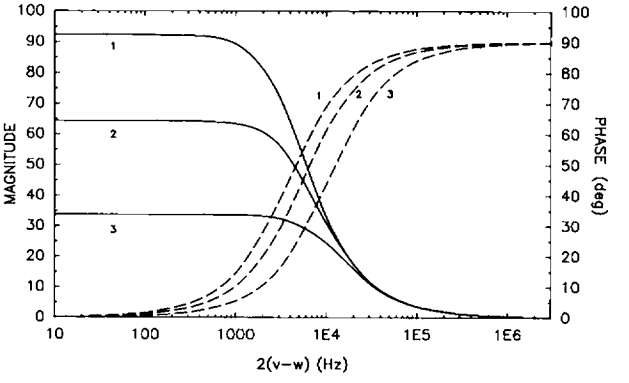

FIGURE 1 Frequency dependence of the phase (*dotted line*) and magnitude (*straight line*) for the sine wave-modulated FPFD fluorescence signal at frequency $2(v-w)$ for three values of τ_r as calculated using Eqs. 35 and 36: 1. $\tau_r = 300\ \mu s$, 2. $\tau_r = 200\ \mu s$, 3. $\tau_r = 100\ \mu s$ and in all cases the triplet lifetime $\tau_\ell = 2$ ms. The phase is expressed in degrees, the magnitude in arbitrary units, and the reference frequency $2(v-w)$ is expressed in hertz.

techniques are not as similar as might appear at first sight. In phase fluorescence methods, fluorescence occurs only at the intensity modulation frequency v and it is from this signal that fluorescence lifetimes are evaluated. Because our method is a depletion technique involving pump and probe excitation, fluorescence is emitted at frequencies of v and $2v$. It is this latter frequency from which we extract triplet state lifetimes.

There is essentially no relationship between our method for determining rotational correlation times and the measurement of time-resolved fluorescence anisotropies by phase fluorometry (Lakowicz et al., 1984). In these methods excitation intensity only is modulated, fluorescence emission is at the source modulation frequency, and phase shifts between fluorescence polarized parallel and perpendicular to the excitation beam are measured to obtain time-resolved anisotropies. We simultaneously modulate both the intensity and polarization of the exciting light at different frequencies to produce triplet state chromophores. Rotational information appears in the fluorescence from remaining singlet chromophores at five combinations and overtones of the intensity and polarization modulation frequencies. In phase fluorometry, there is only one fluorescence frequency v and the $2(v - w)$ combination frequency we use to obtain rotational information optically heterodyned into a lower region of the frequency spectrum has no analog whatsoever.

Although the theoretical development of equations describing sine wave-modulated FPFD experiments is straightforward, the practical task of generating appropriate control signals is very difficult. One requires three sine waves at frequencies corresponding to v, $2v$ and $2(v - w)$, and one triangular wave corresponding to w. All frequencies must be phase coherent and simultaneously variable to allow measurements of fluorescence signals as functions of reference frequencies. Although such signals can, with sufficient effort, be generated, it is much simpler to approximate the sine waves with square waves which are easily generated with digital divider circuits. We therefore explored the possibility of making these same measurements using square wave modulation which was experimentally feasible using existing hardware. We next present the mathematical equations for frequency-modulated PFD using square wave modulation.

Square Wave Modulation

Again we consider a spherical particle rotating in a three dimensional isotropic medium with a single rigidly attached fluorophore situated at the origin of a right-handed xyz-coordinate system. The light travels along the x-axis and the unmodulated intensity I_0 is chopped with a square wave at a frequency v. The polarization is also square wave-modulated at a different frequency w and is either linearly polarized parallel to the z-axis (*vertical*) or to the y-axis (*horizontal*). It is necessary to assume at the outset a specific relation between v and w. For reasons to be discussed later, we choose $w = 5v/4$ always. As shown in Fig. 2, a measurement period consists of 12 intervals of three types: nonilluminated (*dark, D*), illuminated with the polarization vertical (*vertical, V*), and illuminated with the polarization horizontal (*horizontal, H*). The order of these intervals is *V, H, D, V, H, D, H, V, D, H, V,* and *D*; and we designate them by integers i from 0 to 11, respectively.

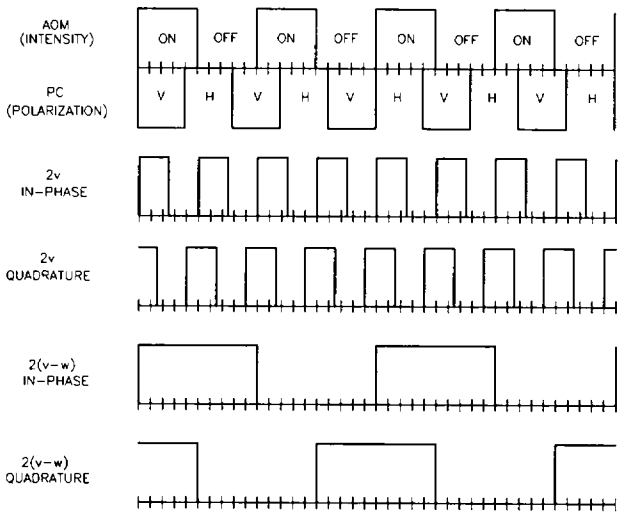

FIGURE 2 Schematic for square wave-modulated FPFD showing the relative relationships of the intensity, polarization, and reference signals as functions of time. The intensity of the light (either on or off) is modulated by an AOM at frequency v. The polarization (either vertical or horizontal) is modulated by a Pockels cell at frequency w. For the case illustrated $1/v = 10$ units, $1/w = 8$ units and one complete measurement period $T = 40$ units. The in-phase or quadrature components for the lifetime- $(2v)$ or rotation-$(2[v - w])$ dependent signal can be isolated with the appropriate demodulator function shown below.

We now proceed to solve the diffusion equation for each interval, subject to the boundary conditions that the distribution function be continuous from interval to interval and periodic after five cycles of v or, equivalently, four cycles of w. The spatial light polarization for a vertically polarized interval is

$$R(\theta, \phi, t) = \cos^2 \theta \tag{37}$$

and, for a horizontally polarized interval, is

$$R(\theta, \phi, t) = \sin^2 \theta \cos^2 \phi. \tag{38}$$

These functions can be expressed in terms of Legendre polynomials in $\cos \theta$ giving

$$R(\theta, \phi, t) = \frac{1}{3} P_0 + \frac{2}{3} P_2 \qquad \text{(vertical intervals);} \tag{39}$$

$$= \frac{1}{3} P_0 - \frac{1}{3} P_2 + \frac{1}{6} P_2^2 \cos 2\phi$$

$$\text{(horizontal intervals).} \tag{40}$$

Both the distribution function $S(\theta, \phi, t)$ and the light

function $P(\theta, \phi, t)$ are then expanded in the eigenfunctions of the Laplacian giving

$$S(\theta, \phi, t) = \frac{1}{4\pi}\left[1 - \sum s_n^m(t)\, P_n^m \cos m\phi\right], \qquad (41)$$

and

$$P(\theta, \phi, t) = I_0 \Sigma\, r_n^m(t)\, P_n^m \cos m\phi, \qquad (42)$$

where the coefficients $s_n^m(t)$ and $r_n^m(t)$ are functions only of time, and P_n^m are the associated Legendre polynomials in $\cos\theta$. We note that $r_n^m(t)$ is a constant within any particular interval since both the light intensity and polarization are constant. Substituting Eqs. 41 and 42 into Eq. 5 gives the time evolution of the distribution function within any interval i:

$$s_n^m(t) = \left[s_n^m(0)\frac{\exp(-k_n t)}{1 - \exp(-k_n T)} + s_n^m(t_i)\right]\exp[-k_n(t - t_i)] + r_n^m(t_i)\, I_0 \frac{\beta}{k_n}\{1 - \exp[-k_n(t - t_i)]\}, \qquad (43)$$

where $s_n^m(t_i)$ are the values of the coefficients at the beginning of the *ith* interval, $s_n^m(0)$ are constants, T is one measurement period, $k_n = k_f$ for $n = 0$, and $k_n = k_c$ for $n = 2$.

Substituting the expression for $s_n^m(t)$ from Eq. 43 and values for $r_n^m(t_i)$ from Eqs. 39 and 40 into Eq. 41 gives

$$S(\theta, \phi, t) = \frac{1}{4\pi}\{1 - [s_0' + s_0(t_i)]P_0 \exp[-k_f(t - t_i)] - [s_2' + s_2(t_i)]P_2 \exp[-k_c(t - t_i)] - [s_2'^2 + s_2^2(t_i)]P_2^2 \cos 2\phi \exp[-k_c(t - t_i)]\} \qquad (\textit{dark intervals}); \quad (44)$$

$$= \frac{1}{4\pi}\Big(1 - [s_0' + s_0(t_i)]P_0 \exp[-k_f(t - t_i)] - [s_2' + s_2(t_i)]P_2 \exp[-k_c(t - t_i)] - [s_2'^2 + s_2^2(t_i)]P_2^2 \cos 2\phi \exp[-k_c(t - t_i)]\} - \frac{1}{3}P_0 I_0 \frac{\beta}{k_f}\{1 - \exp[-k_f(t - t_i)]\} - \frac{2}{3}P_2 I_0 \frac{\beta}{k_c}\{1 - \exp[-k_c(t - t_i)]\}\Big) \qquad (\textit{vertical intervals}); \quad (45)$$

$$= \frac{1}{4\pi}\Big(1 - [s_0' + s_0(t_i)]P_0 \exp[-k_f(t - t_i)] - [s_2' + s_2(t_i)]P_2 \exp[-k_c(t - t_i)] - [s_2'^2 + s_2^2(t_i)]P_2^2 \cos 2\phi \exp[-k_c(t - t_i)]\} - \frac{1}{3}P_0 I_0 \frac{\beta}{k_f}\{1 - \exp[-k_f(t - t_i)]\} + \frac{1}{3}P_2 I_0 \frac{\beta}{k_c}\{1 - \exp[-k_c(t - t_i)]\} - \frac{1}{6}P_2^2 \cos 2\phi\, I_0 \frac{\beta}{k_c}\{1 - \exp[-k_c(t - t_i)]\}\Big) \qquad (\textit{horizontal intervals}); \quad (46)$$

where

$$s_n'^m = s_n^m(0)\frac{\exp(-k_n t)}{1 - \exp(-k_n T)}. \qquad (47)$$

The coefficients $s_0(t_i)$, $s_2(t_i)$, and $s_2^2(t_i)$ are evaluated for each interval sequentially by insisting that the distribution function be continuous from one interval to the next. During these calculations the initial coefficients $s_n^m(0)$ are carried as indeterminate constants. Once the evolution of the distribution function up to the end of the measurement period T has been calculated, $s_0(0)$, $s_2(0)$, and $s_2^2(0)$ can be evaluated from the known periodicity of the distribution function by insisting that $s_n^m(0) = s_n^m(T)$. Since w is $5v/4$ the measurement period T is therefore $4/v$ or $5/w$.

The time-dependent fluorescence intensity $I(t)$ is calculated for each interval in Fig. 2 by convolving the singlet distribution function with the light functions in Eq. 42 for illuminated intervals and integrating with respect to the spatial coordinates. Finally, the measured steady-state voltage U corresponding to either the $2v$ lifetime- or $2(v - w)$ rotation-dependent frequency is calculated by convolving the fluorescence intensity with the lock-in amplifier response function $D(t)$ and averaging the results over one period.

$$U = \frac{1}{T}\int_0^T I(t)\, D(t)\, dt. \qquad (48)$$

As is the case with sine wave-modulated FPFD, the frequency at twice the AOM drive frequency contains the most useful triplet lifetime information. Since excitation polarization has no effect on this signal, we assume the polarization to be constant in the vertical orientation. This is experimentally achieved by turning the PC off for the duration of the lifetime experiment. For a conventional lock-in amplifier operated with a reference voltage $E(t)$, the response function $D(t)$ is a symmetric bipolar square

wave at the reference frequency (Princeton Applied Research Corporation, 1977):

$$D(t) = \begin{cases} 1.11 \text{ for } E(t) \geq 0 \\ -1.11 \text{ for } E(t) < 0 \end{cases} \quad (49)$$

The in-phase component U_{2v}(in-phase) of the lifetime-dependent signal is thus

$$U_{2v}(\text{in-phase}) = \frac{1.1}{9k_f^2} I_0^2 \beta B f v' \left(\frac{1 - 2x^2 + x^4}{1 + x^4} \right), \quad (50)$$

where $v' = 2v$ and $x = \exp(-k_f/4v')$.

To calculate the quadrature component of the signal a 90° phase lead is introduced to the response function (Fig. 2) and substituted into Eq. 48. The quadrature component U_{2v}(quad) of the lifetime signal is

$$U_{2v}(\text{quad}) = \frac{1.1}{9k_f^2} I_0^2 \beta B f v' \left(\frac{1 - 2x + 2x^3 - x^4}{1 + x^4} \right). \quad (51)$$

Similarly, the rotation-dependent signal can be calculated. As in the case of sine wave-modulated PFD the most useful signal lies at $2(v - w)$. Various criteria were developed to determine the most suitable combination of v and w (see Results and Discussion). It was found that the most practical choice was $w = 5v/4$. For this particular frequency combination, the in-phase and quadrature signals are identical and we evaluate a single rotation-dependent signal $U_{2(v-w)}$ at frequency $2(v - w)$. This signal is

$$\begin{aligned} U_{2(v-w)} = -\frac{4.44}{15k_c^2} I_0^2 \beta B f v' \left(\frac{1}{1 + x^{20}} \right) (x - x^2 - x^3 + x^4 \\ + x^5 - x^6 - x^7 + x^8 - x^9 \\ + 2x^{10} - x^{11} + x^{12} - x^{13} \\ - x^{14} + x^{15} - x^{16} + x^{17} + x^{18} - x^{19}), \end{aligned} \quad (52)$$

where $x = \exp(-k_c/20v')$, and $v' = 2(v - w)$.

METHODS AND MATERIALS

Instrumentation

The instrumentation used for time domain PFD measurements (Yoshida and Barisas, 1986) is easily modified for frequency domain measurements. A block diagram of the system is shown in Fig. 3. As stated in the Theory section, while sine wave modulation is easier to develop theoretically and potentially more efficient, the procedure is very difficult to implement instrumentally. Therefore our experimental system is based on square wave modulation of the light intensity, polarization, and reference signals. The system consists of a Coherent Radiation Innova 90 argon ion laser (Coherent Inc., Laser Division, Palo Alto, CA) operated with a TEM 00 power of 100 mW at 514.5 nm. The vertically polarized output enters a Lasermetric 3031 transverse Pockels cell (Lasermetric Inc., Teaneck, NJ) which is driven by special AC-MOSFET driver. In response to a square wave input the PC rotates the plane of polarization of light by 90° within a frequency range of 10 Hz to 1 MHz with a rise and fall time <100 ns. The light then enters a digital acousto-optic modulator (Coherent, Inc. Modulator Division., Danbury, CT). By isolating the

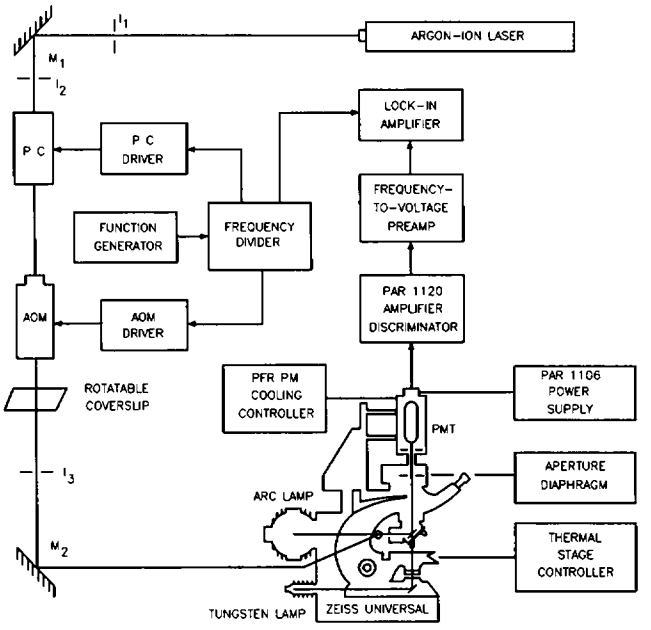

FIGURE 3 Block diagram of polarized fluorescence depletion system. M_1 and M_2 are first surface mirrors. I_1, I_2, and I_3 are iris diaphragms. The functions of all other components are described in the text.

first-order diffracted beam from the AOM with an iris diaphragm, the light intensity can be modulated with an extinction ratio of >1,000:1. The light then passes through a rotatable microscope coverslip which compensates for differences in intensities of the two orthogonal polarizations caused by reflections off various mirrors in the system. After two 90° reflections, the beam enters the horizontal optical port of a Zeiss Universal microscope fitted with a III/RS epifluorescence illuminator (Carl Zeiss Inc., Thornwood, NY). The sample is illuminated on a temperature controlled microscope stage and scattered light is eliminated with a KV 550 barrier filter (Schott Glass Tech. Inc., Duryea, PA). A small portion of the illuminated sample area is isolated with the aperture diaphragm of a Zeiss MP03 photometer and detected with a thermionically-cooled EMI 9816A photomultiplier tube (Thorn EMI Gencom Inc., Plainview, NY) fitted with two focusing ring magnets (Products for Research Inc., Danvers, MA) to reduce dark current. Single-photon pulses are generated with a PAR 1120 amplifier/discriminator (Princeton Applied Research Corp., Princeton, NJ) and are fed into a frequency-to-voltage converter circuit which generates a voltage proportional to the number of photon counts per second. This signal is AC-coupled to the input of a PAR 5203 lock-in amplifier which has a maximum reference frequency of 100 KHz. The reference signals used by the lock-in, along with control signals for the AOM and PC, are generated with a digital divider circuit that divides a square wave from a 2 Hz to 2 MHz function generator (Model 116, Wavetek Corp., San Diego, CA) down to frequencies corresponding to v, $2v$, w, and $2(v - w)$. To insure symmetric square wave outputs, each signal is passed through a divide-by-two counter. A reset circuit is also included to insure phase coherence for all signals.

The actual frequencies used in the experiment are based on a value of w relative to v chosen as described in the Results and Discussion section. This value remained constant at $w = 5v/4$ throughout our experiments. Thus if the light is intensity-modulated at a frequency of v and the polarization is modulated at a frequency of $w = 5v/4$, then the lifetime-dependent signal is $2v$ and the rotation-dependent signal is $2(v - w) = 0.5v$. These four frequencies are obtained by dividing the function generator frequency ν by an appropriate set of integers and then dividing each frequency by two to symmetrize the outputs. For $w = 5v/4$ the results are $v = \nu/20$, $w = \nu/16$, $2v = \nu/10$, and $2(v - w) = \nu/40$.

Dye-Labeled Proteins

Eosin-5'-isothiocyanate (EITC) (Molecular Probes, Junction City, OR) was conjugated to BSA and anaerobic solutions of the protein in glycerol were prepared by a procedure given previously (Yoshida and Barisas, 1986). Equal molar amounts of the protein and dye were reacted in 0.1 M $NaHCO_3$ buffer containing 0.5 M NaCl at pH 8 for 3–6 h at room temperature. Unreacted dye was separated on G-25-150. The solution was then extracted three times with n-butanol (Niswender et al., 1985) to further eliminate unreacted dye hydrophobically bound to the protein (Cherry et al., 1976). The product contained ≈0.7 mol of EITC per mol of BSA. Preparation of protein in glycerol was performed in a nitrogen-filled glove box with the sample sealed on a quartz Supersil II microscope slide (Heraeus Amersil, Inc., Sayreville, NJ) with quick setting epoxy. Final protein concentration was 0.15 mg per gram of glycerol.

RESULTS AND DISCUSSION

To illustrate the various frequency combinations which make up the fluorescence signal, the power spectrum of EITC-labeled BSA in 99% glycerol was obtained (Fig. 4). The sample temperature was 4°C and data were accumulated with a Nicolet 12/70 signal averager at 200 μs/point and with a fundamental AOM frequency v of 1.0 kHz. Fig. 4 shows signal magnitudes plotted versus frequency normalized to v. In Fig. 4 *a* the polarization is modulated at a frequency $w = 5v/4$ producing the sum and difference combinations of v and w. Incomplete balancing of the light intensities having vertical and horizontal polarizations produces a line at 1.250 which corresponds to w. The rotation-dependent signal at $2(v - w)$ is clearly visible at a relative frequency of 0.500 along with the lifetime-dependent signal at $2v$ with a frequency of 2.00. Also present are $v - w$, $v + w$ at frequencies of 0.249 and 2.251, respectively. Other identifiable lines include the odd harmonics of $v - w$ at 0.752, 1.250, and 1.750 and the odd harmonics of $2(v - w)$ at 1.501, and 2.500. To confirm these frequencies are due to mixing of v and w, we obtained another spectrum (Fig. 4 *b*) of the same sample with the polarization constant in the vertical orientation. As can be seen in Fig. 4 *b* all frequencies associated with w are eliminated with the only remaining identifiable lines being v and $2v$. The small lines at 0.180, 0.349, and 1.182 appear in both spectra but are not identifiable.

The presence of harmonics of v and w and of combinations of these frequencies points out fundamental disadvan-

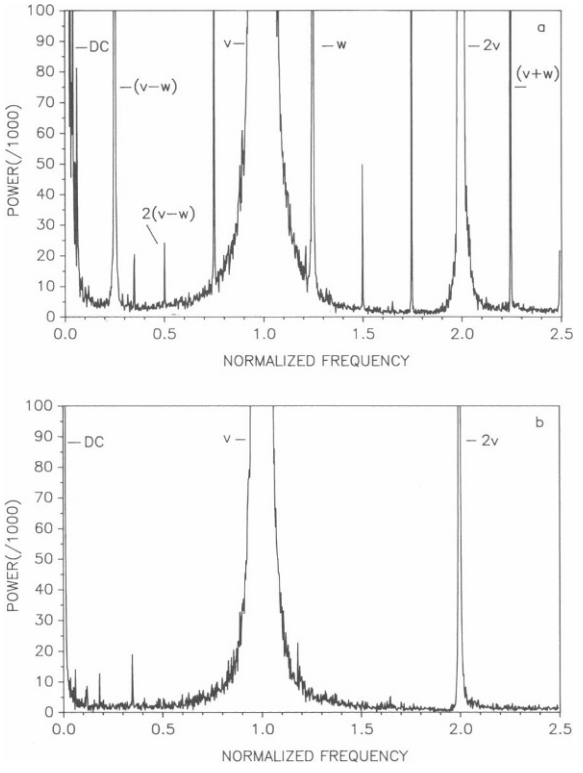

FIGURE 4 Fluorescence power spectrum of EITC-labeled BSA in 99% glycerol showing the various frequency components which make up the fluorescence signal. Data were taken at 200 μs/point with v = 1 kHz and w = 1.25 kHz. Signal magnitudes are plotted versus frequencies normalized to v. (*a*) Frequency spectrum where the exciting light is intensity modulated at frequency v and polarization modulated at a different frequency w. All identifiable combination and overtones of v and w predicted by theory are labeled. (*b*) Frequency spectrum where only the intensity of the exciting light was modulated at frequency v. The polarization was kept constant in the vertical orientation.

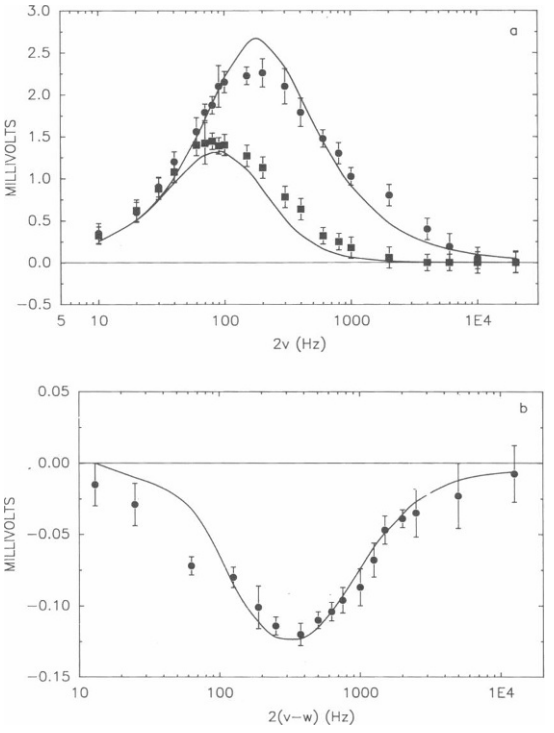

FIGURE 5 (*a*) Frequency dependence for the in-phase (*circles*) and quadrature (*squares*) components of the lifetime-dependent fluorescence signal at frequency $2v$ for EITC-labeled BSA in 99% glycerol at 0°C. The polarization is kept constant in the vertical orientation. (*b*) Frequency dependence of the rotation-dependent signal at frequency $2(v - w)$ for the same sample, where the intensity is modulated at frequency v and the polarization is modulated at a frequency $w = 5v/4$. Both in-phase and quadrature signals were averaged and the error bars represent ±1 standard error of the mean for 6 to 10 measurements. In both *a* and *b* the solid lines represent theoretical calculations using Eqs. 50–52.

tages of square wave-modulated FPFD relative to sine wave-modulated FPFD. In sine wave-modulated FPFD all the signal power will be concentrated in five discrete frequencies including $2(v - w)$. In square wave modulation the signal power will be spread over the odd harmonics of $2(v - w)$ and other combination frequencies resulting from the convolution of square wave harmonics with one another. Since real biological systems frequently consist of only some thousands of fluorescent molecules, only limited total signal can be obtained. It is therefore of great importance to concentrate the signal into a few discrete frequencies. Filtering a square wave-modulated signal to isolate the $2(v - w)$ line is thus not a satisfactory solution since much of the rotation information, being distributed among other frequencies, is lost.

To test the equations we developed for square wave-modulated FPFD we measured both the lifetime and rotation signals as functions of frequency for EITC labeled BSA in 99% glycerol. The concentration of the protein was 0.015% (wt/wt) and the temperature was 0°C. The steady-state depletion was <15% and the RMS voltage U_v at the AOM fundamental frequency v was 70 mV. Fig. 5 *a* shows the lifetime-dependent in-phase and quadrature signals at frequency $2v$ and Fig. 5 *b* shows the average for the single in-phase and quadrature rotation-dependent signal at frequency $2(v - w)$. In all cases the signal intensity in millivolts is plotted versus the reference frequency in Hertz. As discussed before the Pockels cell was turned off when the lifetime-dependent signal at $2v$ was measured. This amounts to holding the polarization constant in the vertical orientation which is the way the Eqs. 50 and 51 were derived. The solid lines represent calculated data using Eqs. 50 and 51 for the $2v$ signal and Eq. 52 for the $2(v - w)$ signal. By means of a nonlinear least squares algorithm (Barisas and Gill, 1979), the three data sets were globally analyzed to obtain the parameters $\beta I_0^2 Bf$, the triplet lifetime, and the rotational correlation time. The results for the fit were $\beta I_0^2 Bf = 6.75 \pm 0.03 \times 10^4$ mV s^{-1}, $\tau_R = 1.84 \pm 0.01$ ms and $\tau_r = 492 \pm 37$ μs. The standard error for the overall fit was ±0.16 mV for the lifetime-dependent signal and ±0.018 mV for the rotation-dependent signal. These values are in good agreement with the measured uncertainties of individual data points (Fig. 5). The slight apparent broadening of the data peaks for both the lifetime and rotation-dependent signals relative to theoretical predictions probably arises from multiple excited state decay processes and rotational correlation times, respectively. For EITC-concanavalin A Austin et al. (1979) report two triplet lifetimes each having appreciable amplitudes. In aqueous solution BSA is most closely approximated by a prolate ellipsoid of axial ratio $a/b = 3.5$ (Squire et al., 1968) and should, therefore, exhibit at least two rotational correlation times. All three observed curves in Fig. 5 would thus be expected to be somewhat broader than predicted by simple theory. This is what is observed qualitatively.

To compare FPFD against a technique known to give accurate results under similar conditions, time domain PFD measurements on the same sample were made just after the frequency domain measurements. A triplet lifetime of 1.43 ± 0.10 ms and a rotational correlation time of 532 ± 38 μs were determined. Since time domain PFD measurements have an overall accuracy of ~±10% (Yoshida and Barisas, 1986), the time domain and frequency domain results are in very good agreement.

The fitted parameter $\beta I_0^2 Bf$ in Eqs. 50–52 relates the magnitude of the lifetime and rotation-dependent signals to measurable properties of the excitation source power and geometry and thus provide a means to check the accuracy of the measured signal. For a Gaussian laser beam with power P and $1/e^2$ radius w

$$\beta I_0^2 Bf = \beta B\sigma \frac{P^2}{\pi w^2}, \tag{53}$$

where σ is the spatial concentration of chromophores in particles/cm^2. The parameter β can be calculated from known constants using Eq. 6. For EITC values of $\epsilon_M^{514} = 46 \times 10^3$ M^{-1} cm^{-1} and $\Phi_t = 0.71$ (Johnson and Garland, 1982) give $\beta = 968$ cm^2 W^{-1} s^{-1}. The constants $B\sigma$ in Eq. 53 are related to the RMS voltage U_v observed at low frequencies v by

$$U_v = \frac{1.11 B\sigma P}{6}. \tag{54}$$

For this experiment $U_v = 70$ mV and $P = 25$ μW so $B\sigma = 1.5 \times 10^7$ mV W^{-1}. Substituting this value into Eq. 53 and $w = 57$ μm gives $\beta I_0^2 Bf = 8.95 \times 10^4$ mV s^{-1}, which agrees well with the value obtained from the least squares fit of the experimental data. Therefore the theoretical equations developed for square wave-modulated FPFD predict both the frequency-dependent behavior and the magnitudes of the observed signals.

As mentioned in the Theory section the synthesis of phase coherent sine wave drive signals is a difficult task, whereas the generation of the equivalent square waves is relatively simple. Unfortunately the use of square waves as drive signals causes some significant problems. In order to minimize these problems, criteria were developed to select optimum relative values of v and w. The first consideration is that the frequencies of the two drive signals should be as close to each other as possible. This allows the difference frequency $2(v - w)$ to be heterodyned to a region of the frequency spectrum below the fundamentals and their harmonics, thus eliminating potential interference from such signals. The second consideration is that neither the fundamental frequencies v and w nor their harmonics overlap the odd harmonics of the rotation-dependent signal at $2(v - w)$. Since the lock-in amplifier uses a square wave demodulator, it is sensitive to odd *nth* harmonics of the reference frequency with a response proportional to $1/n$. The odd harmonics of the frequencies v and w appear in the

fluorescence signal with more than enough intensity to interfere with the $2(v - w)$ signal through this mechanism. If one examines Fig. 2 it is apparent that information about rotational relaxation is only available when the polarization changes during an illuminated interval. Therefore a third criterion is that the Pockels cell should be modulated at a higher frequency than the AOM, thus producing changes in the polarization during each illuminated interval. Finally, the complexity of developing the equations to describe FPFD signals must also be considered in choosing values of v and w. For example, if $w = 5v/4$ (Eq. 52), there are 20 exponential terms to be calculated. If $w = 7v/8$, there are 56 terms; and, if $w = 9v/8$, there are 72 terms. By this latter point a closed-form analytical description of the experiment is no longer practical.

The main sources of error encountered for FPFD are fluctuations of the lock-in amplifier signal during the 30 s integration period. Even with these long integration times, the noise levels were $\approx$10–15% of the signal amplitude. It is not likely that these fluctuations were caused by laser instability even though the signal is proportional to the square of the input intensity. Fluctuations of the laser while in the light control mode are $<\pm 0.5\%$. It is more likely that these problems were due to overall amplifier stability, amplifier noise, and background noise such as ground loops. All of these factors are reflected in the uncertainty in the measurements of individual data points shown in Fig. 5 where the error bars represent ± 1 standard error of the mean for 6 to 10 measurements. Irreversible sample photobleaching was very slow relative to the microsecond timescale processes studied and probably has little effect on signal stability. A maximum of 25% of the sample was irreversibly photobleached during the 30 to 60 s it was observed. A final concern in PFD measurements is the possibility of laser-induced sample heating. To calculate the temperature increase expected in FPFD experiments, we used equations for laser-induced heating developed before (Yoshida and Barisas, 1986). We calculated a rise in sample temperature of <0.1°C during the illuminated intervals for a laser power of 40 μW, a beam radius of 50 μm and a sample thickness of 0.1 mm. Laser-induced sample heating is therefore neither a problem in frequency domain PFD nor in time domain PFD.

In summary we have presented the theory for a new technique for measuring slow rotational motion using sine wave-modulated frequency domain PFD. This technique shows promise in that the theoretical development is straightforward and simple equations can be derived to describe experimental data. Also, the technique is interesting in that, by manipulating certain frequency combinations in the system, we can heterodyne the signal of interest into a low frequency region of the spectrum relatively free from noise and interfering signals. Unfortunately implementation of sine wave-modulated PFD measurements was not possible using available instrumentation. Therefore we developed the mathematical models for, and built an experimental system based on, square wave modulation. We were thus able to demonstrate the basic feasibility of FPFD measurement of the rotational diffusion of BSA in glycerol. The mathematical models were shown to adequately fit the observed data and independent measurements on the same sample using time domain PFD was shown to agree with results obtained from frequency domain PFD. Further studies involving sine wave-modulated FPFD are in progress.

Supported by National Science Foundation grant PCM 84-10763 and National Institutes of Health grant AI-21873.

Thomas Yoshida is supported in part by a fellowship from the Proctor and Gamble Company.

Received for publication 30 March 1988 and in final form 1 April 1988.

REFERENCES

Austin, R. H., S. S. Chen, and T. M. Jovin. 1979. Rotational diffusion of cell surface components by time-resolved phosphorescence anisotropy. *Proc. Natl. Acad. Sci. USA.* 76:5650–5654.

Barisas, B. G., and S. J. Gill. 1979. Thermodynamic analysis of carbon monoxide binding to trout hemoglobin. I. *Biophys. Chem.* 9:235–244.

Cherry, R. J., A. Cogoli, M. Oppliger, G. Schneider, and G. Semenza. 1976. A spectroscopic technique for measuring slow rotational diffusion of macromolecule. 1: Preparation and properties of a triplet probe. *Biochemistry.* 15:3653–3656.

Cherry, R. J., and J. Schneider. 1976. A spectroscopic technique for measuring slow rotational diffusion of macromolecules. 2: Determination of rotational correlation time of proteins in solution. *Biochemistry.* 15:3657–3661.

Cherry, R. J. 1979. Rotational and lateral diffusion of membrane proteins. *Biochim. Biophys. Acta.* 559:289–327.

Chong, P. L. G., A. R. Cossins, and G. Weber. 1983. A differential polarized phase fluorometric study of the effects of high hydrostatic pressure upon the fluidity of cellular membranes. *Biochemistry.* 22:409–415.

Garland, P. B., and C. A. Moore. 1979. Phosphorescence of protein-bound eosin and erythrosin. *Biochem. J.* 183:561–572.

Garland, P. B., and J. J. Birmingham. 1986. Triplet probes and the rotational diffusion of membrane proteins. *In* Applications of Fluorescence in the Biomedical Sciences. D. L. Taylor, F. Lanni, and A. S. Waggoner, editors. Alan R. Liss Inc., New York. Chap. 11.

Gratton, E., D. M. Jameson, and R. D. Hall. 1984. Multifrequency phase and modulation fluorometry. *Ann. Rev. Biophys. Bioeng.* 13:105–124.

Gratton, E., and D. M. Jameson. 1985. New approach to phase and modulation resolved spectra. *Anal. Chem.* 57:1694–1697.

Jameson, D. M., E. Gratton, and R. D. Hall. 1984. The measurement and analysis of heterogeneous emissions by multifrequency phase and modulation fluorometry. *Appl. Spectrosc. Rev.* 20:55–106.

Johnson, P., and P. B. Garland. 1982. Fluorescent triplet probes for measuring the rotational diffusion of membrane proteins. *Biochem. J.* 203:313–321.

Keating-Nakamoto, S., H. Cherek, and J. R. Lakowicz. 1985. A new method for resolution of two- and three-component mixtures of fluorophores by phase-sensitive detection of fluorescence. *Anal. Biochem.* 148:349–356.

Lakowicz, J. R., and F. G. Prendergast. 1978. Detection of hindered rotations of 1,6-diphenyl-1,3,5-hexatriene in lipid bilayers by differential polarized phase fluorometry. *Biophys. J.* 24:213–231.

Lakowicz, J. R., F. G. Prendergast, and D. Hogen. 1979. Differential polarized phase fluorometric investigations of diphenylhexatriene in

lipid bilayers. Quantitation of hindered depolarizing rotations. *Biochemistry*. 18:508–519.

Lakowicz, J. R., and R. B. Thompson. 1983. Differential polarized phase fluorometric studies of phospholipid bilayers under high hydrostatic pressure. *Biochim. Biophys. Acta*. 732:359–371.

Lakowicz, J. R., E. Gratton, H. Cherek, B. P. Maliwal, and G. Laczko. 1984. Determination of time-resolved fluorescence emission spectra and anisotropies of a fluorophore-protein complex using frequency-domain phase-modulation fluorometry. *J. Biol. Chem.* 259:10967–10972.

Lakowicz, J. R., and B. P. Maliwal. 1985. Construction and performance of a variable-frequency phase-modulation fluorometer. *Biophys. Chem.* 21:61–78.

Lakowicz, J. R., H. Cherek, B. P. Maliwal, and E. Gratton. 1985. Time-resolved fluorescence anisotropies of diphenylhexatriene and perylene in solvents and lipid bilayers obtained from multifrequency phase-modulation fluorometry. *Biochemistry*. 24:376–383.

Mantulin, W. W., and G. Weber. 1977. Rotational anisotropy and solvent-fluorophore bonds: an investigation by differential polarized phase fluorometry. *J. Chem. Phys.* 66:4092–4099.

Moore, C., D. Boxer, and P. B. Garland. 1979. Phosphorescence depolarization and the measurement of rotational motion of proteins in membrane. *FEBS (Fed. Eur. Biochem. Soc.) Lett.* 108:161–166.

Mousa, J. J., and J. D. Winefordner. 1974. Phase resolved phosphorimetry. *Anal. Chem.* 46:1195–1209.

Niswender, G. D., D. A. Roess, H. R. Sawyer, W. Silvia, and B. G. Barisas. 1985. Difference in the lateral mobility of receptors for LH in the luteal cell plasma membrane when occupied by oLH vs. hCG. *Endocrinology*. 116:164–169.

Princeton Applied Research Corporation. 1977. *Model 5203 Lock-in Amplifier*. p. IV–14.

Squire, P. G., P. Moser, and C. T. O'Konski. 1968. The hydrodynamic properties of bovine serum albumin monomers and dimer. *Biochemistry*. 7:4261–4272.

Valeur, B., and G. Weber. 1977. Anisotropic Rotation in 1-naphthylamine existence of a red-edge transition moment normal to the ring plane. *Chem. Phys. Lett.* 45:140–144.

Weber, G., S. L. Helgerson, W. A. Cramer, and G. W. Mitchell. 1976. Change in rotational motion of a cell-bound fluorophore caused by colicin E1: a study by fluorescence polarization and differential polarized phase fluorometry. *Biochemistry*. 15:4429–4432.

Yoshida, T. M., and B. G. Barisas. 1986. Protein rotational motion in solution measured by polarized fluorescence depletion. *Biophys. J.* 50:41–53.